

Copper(II) and Copper(III) Complexes of Pyrrole-Appended Oxacarboxyporphyrin

Miłosz Pawlicki, Izabela Kańska, and Lechosław Latos-Grażyński*

Department of Chemistry, University of Wrocław, 14 F. Joliot-Curie Street, Wrocław 50 383, Poland

Received April 3, 2007

The reaction of an *O*-confused porphyrin with a pendant pyrrole **4** and copper(II) acetate yields an organocopper(III) diamagnetic complex **4-Cu(III)** substituted at the C(3) position by the pyrrole and H. The transformation of **4-Cu(III)**, performed in aerobic conditions, gave a rare copper(II) organometallic compound **6-Cu(II)**. In the course of this process, the tetrahedral–trigonal rearrangement originated at the C(3) atom but effects the whole structure. The electron paramagnetic resonance spectroscopic features correspond to a copper(II) oxidation state. A crystallographic analysis of **6-Cu(II)** confirmed the formation of a direct metal–C bond [Cu(II)–C 1.939(4) Å]. It was found that the Cu(II) complex of *O*-confused oxaporphyrin is sensitive to oxidative conditions. The degradation of **6-Cu(II)** to yield copper(II) tripyrri-*none* complexes has been observed, which was considered as a peculiar case of dioxygen activation in a porphyrin-like environment. This process is accompanied by regioselective oxygenation at the inner C to form the 2-oxa-3-(2'-pyrrolyl)-21-hydroxycarboxyporphyrinatocopper(II) complex ((pyrr)OCPO)Cu^{II} (**8**). The reaction of **6-Cu(II)** with hydrogen peroxide, performed under heterophasic conditions, resulted in quantitative regioselective hydroxylation centered at the internal C(21) atom, also producing **8**. Treatment of **8** with acid results in demetalation to form the nonaromatic 21-hydroxy *O*-confused porphyrin derivative ((pyrr)OCPOH)H (**9**).

Introduction

A heteroatom confusion (*X*-confusion) concept, first exemplified by a porphyrin–2-aza-21-carboxyporphyrin couple **1**,^{1,2} corresponds formally to an interchange of a heteroatom with a β -methine group, i.e., to a step that transforms the regular 21-*X*-heteroporphyrin into its “*X*-confused” isomer.^{3,4} This strategy resulted in the formation of thia- **2**^{5–7} and oxa analogues **3**^{8,9} of *N*-confused porphyrin **1**, where the S or O atoms are placed at the macrocyclic perimeter. The C atom of the heterocyclic subunit is directed toward the center of the macrocyclic crevice (Chart 1).

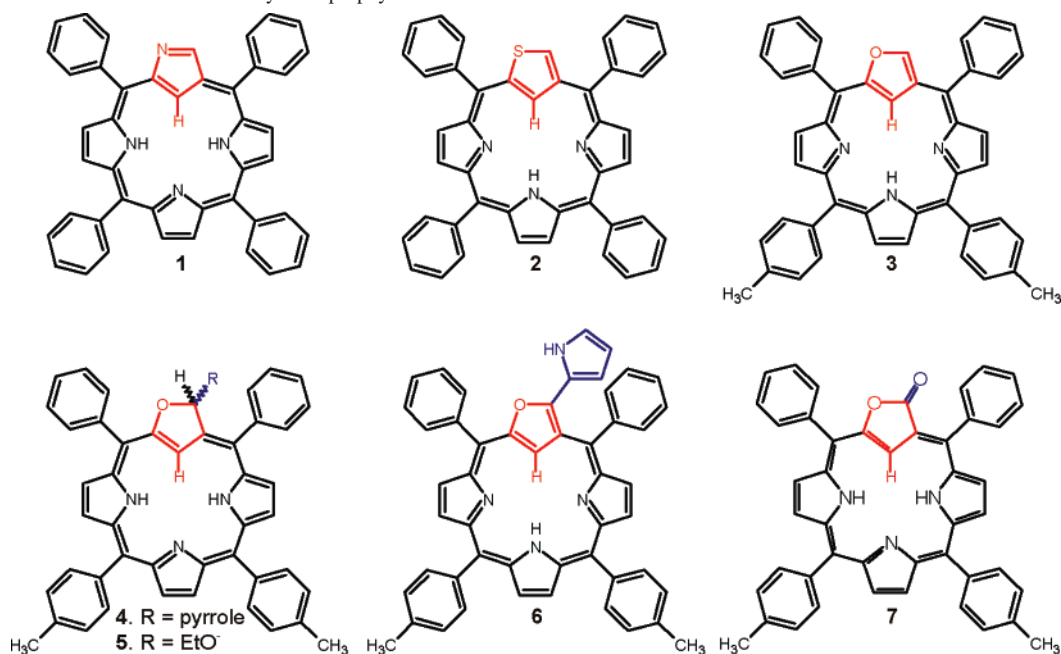
Following such an approach, we have characterized *O*-confused oxaporphyrin **3**, albeit in its dicationic form,⁸ and *S*-confused thiaporphyrin **2**.⁵ In contrast to *S*-confused thiaporphyrin **2**, the oxa analogue **3** is extremely reactive toward nucleophilic attack at peripheral position 3, which results in aromatization of the macrocycle and the formation of derivatives like **4** and **5**, both formally related to the product of 2-oxa-21-carboxyporphyrin hydrogenation.^{8,9} Thus, the macrocyclic delocalization and aromaticity in **3** is easily switched on and off by reversible addition/elimination of a nucleophile at the position C(3), coupled with tetrahedral–trigonal conversion of C(3). Notably, oxidation of the hydroxy analogue of **5** yields carbaporpholactone **7**, which contains the lactone functionality instead of the regular furan moiety.⁸

In general, syntheses of carbaporphyrinoids, including those obtained following the *X*-confusion approach,³ allow an exploration of organometallic chemistry in a porphyrin-

* To whom correspondence should be addressed. E-mail: llg@wchuwr.chem.uni.wroc.pl.

- (1) Chmielewski, P. J.; Latos-Grażyński, L.; Rachlewicz, K.; Głowiak, T. *Angew. Chem., Int. Ed. Engl.* **1994**, *33*, 779.
- (2) Furuta, H.; Asano, T.; Ogawa, T. *J. Am. Chem. Soc.* **1994**, *116*, 767.
- (3) Pawlicki, M.; Latos-Grażyński, L. *Chem. Rec.* **2006**, *6*, 64.
- (4) Furuta, H.; Maeda, H.; Osuka, A. *Chem. Commun.* **2002**, 1795.
- (5) Sprutta, N.; Latos-Grażyński, L. *Tetrahedron Lett.* **1999**, *40*, 8457.
- (6) Chmielewski, M. J.; Pawlicki, M.; Sprutta, N.; Sztrenberg, L.; Latos-Grażyński, L. *Inorg. Chem.* **2006**, *45*, 8664.
- (7) Sztrenberg, L.; Sprutta, N.; Latos-Grażyński, L. *J. Inclusion Phenom.* **2001**, *41*, 209.
- (8) Pawlicki, M.; Latos-Grażyński, L. *J. Org. Chem.* **2005**, *70*, 9123.
- (9) Pawlicki, M.; Latos-Grażyński, L. *Chem.—Eur. J.* **2003**, *9*, 4650.

- (10) Latos-Grażyński, L. Core-Modified Heteroanalogues of Porphyrins and Metalloporphyrins. In *The Porphyrin Handbook*; Kadish, K. M., Smith, K. M., Guilard, R., Eds.; Academic Press: New York, 2000; Vol. 2, Chapter 14, pp 361–416.
- (11) Harvey, J. D.; Ziegler, C. J. *Coord. Chem. Rev.* **2003**, *247*, 1.

Chart 1. Selected X-Confused *meso*-Tetraarylcarbaporphyrinoids

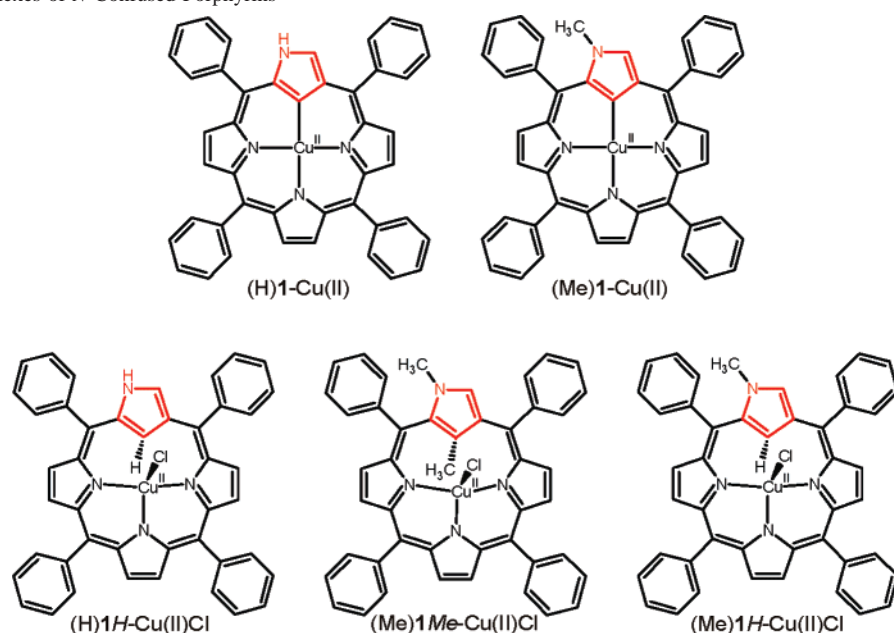
like environment. Therefore, the coordination properties of the first reported carbaporphyrinoid (*N*-confused carbaporphyrin) **1** have been studied for a large variety of metal ions.^{4,10–15} The remarkable flexibility of the *N*-confused porphyrin is reflected by the formation of various coordination modes in macrocyclic environments, with or without the formation of a direct metal–C bond.^{1,16,17} Importantly, atypical oxidation states of metal ions trapped in organometallic environments have been identified.^{18–24} The coordination properties were also explored for carbocyclic analogues as exemplified by *m*-benzporphyrin,^{25–28} azulporphyrin,²⁹ and benzocarboraphyrin.³⁰

The coordination chemistry of *O*-confused oxaporphyrins has been reported for a limited number of metal ions. The reported coordination features resemble those of *N*-confused porphyrins. Thus, an insertion of metal ions into *O*-confused oxaporphyrin derivatives afforded organometallic complexes of **3** (Ag(III)),⁸ **4** (Ag(III)),⁹ **5** (Ag(III)),⁸ **6** (Ag(III), Ni(II), and Pd(II))⁹ and **7** (Ag(III)).⁸ Significantly, an accommodation of Ni(II) or Pd(II) by **4** is linked to a dehydrogenation step, which results in the formation of a “true” *O*-confused oxaporphyrin frame of **6** but with a pendant pyrrole. The pyrrole-appended *O*-confused oxaporphyrin **6** acts also as a monoanionic ligand toward Zn(II) and Cd(II) cations. Three N atoms and the C(21)H fragment of the inverted furan occupy equatorial positions. The proximity of the furan fragment to the metal ion induces direct scalar couplings between the spin-active nucleus of the metal (^{111/113}Cd) and the adjacent ¹H nucleus.³¹

In light of these observations, we have turned our attention to organocopper chemistry of the *O*-confused porphyrin macrocycle. In general, the organometallic chemistry of copper is nearly exclusively focused on the metal oxidation state +1.³² Electron-rich organocopper(I) compounds are widely applied as useful reagents in numerous organic syntheses.³³ Transient organocopper(III) species were considered in the mechanism of a multiple bond activation *via* reactive π complexes. Their transformations into the σ -carbon copper(III) intermediates were followed by reductive elimination.^{34–37} It was also demonstrated that doubly

- (12) Srinivasan, A.; Furuta, H. *Acc. Chem. Res.* **2005**, *38*, 10.
 (13) Chmielewski, P. J.; Latos-Grażyński, L. *Coord. Chem. Rev.* **2005**, *249*, 2510.
 (14) Harvey, J. D.; Ziegler, C. J. *J. Inorg. Biochem.* **2006**, *100*, 869.
 (15) Maeda, H.; Furuta, H. *Pure Appl. Chem.* **2006**, *78*, 29.
 (16) Chmielewski, P. J.; Latos-Grażyński, L.; Głowiak, T. *J. Am. Chem. Soc.* **1996**, *118*, 5690.
 (17) Furuta, H.; Morimoto, T.; Osuka, A. *Inorg. Chem.* **2004**, *43*, 1618.
 (18) Chmielewski, P. J.; Latos-Grażyński, L. *Inorg. Chem.* **1997**, *36*, 840.
 (19) Furuta, H.; Ogawa, T.; Uwatoko, Y.; Araki, K. *Inorg. Chem.* **1999**, *38*, 2676.
 (20) Chmielewski, P. J.; Latos-Grażyński, L.; Schmidt, I. *Inorg. Chem.* **2000**, *39*, 5475.
 (21) Chmielewski, P. J.; Latos-Grażyński, L. *Inorg. Chem.* **2000**, *39*, 5639.
 (22) Rachlewicz, K.; Wang, S.-L.; Ko, J.-L.; Hung, C.-H.; Latos-Grażyński, L. *J. Am. Chem. Soc.* **2004**, *126*, 4420.
 (23) Maeda, H.; Osuka, A.; Ishikawa, Y.; Aritome, I.; Hisaeda, Y.; Furuta, H. *Org. Lett.* **2003**, *5*, 1293.
 (24) Bohle, D. S.; Chen, W.-C.; Hung, C.-H. *Inorg. Chem.* **2002**, *41*, 3334.
 (25) Stępień, M.; Latos-Grażyński, L. *Acc. Chem. Res.* **2005**, *38*, 88.
 (26) Hung, C.-H.; Chang, F.-C.; Lin, C.-Y.; Rachlewicz, K.; Stępień, M.; Latos-Grażyński, L.; Lee, G.-H.; Peng, S.-M. *Inorg. Chem.* **2004**, *43*, 4118.
 (27) Stępień, M.; Latos-Grażyński, L.; Sztterenber, L.; Panek, J.; Latajka, Z. *J. Am. Chem. Soc.* **2004**, *126*, 4566.
 (28) Stępień, M.; Latos-Grażyński, L. *Chem.—Eur. J.* **2001**, *7*, 5113.
 (29) Lash, T. D.; Colby, D. A.; Graham, S. R.; Ferrence, G. M.; Szczepura, L. F. *Inorg. Chem.* **2003**, *42*, 7326.
 (30) Lash, T. D.; Rasmussen, J. M.; Bergman, K. M.; Colby, D. A. *Org. Lett.* **2004**, *6*, 549.

- (31) Pawlicki, M.; Latos-Grażyński, L.; Sztterenber, L. *Inorg. Chem.* **2005**, *44*, 9779.
 (32) van Koten, G.; James, S. L.; Jastrzebski, J. T. B. H. In *Comprehensive Organometallic Chemistry II*; Wardell, J. L., Abel, E. W. W., Stone, F. G. A., Wilkinson, G., Eds.; Elsevier Science Ltd.: London, 1995; Chapter 3.
 (33) *Organocopper Reagents*; Taylor, R. J. K., Ed.; Oxford University Press: Oxford, U.K., 1994.
 (34) Chouan, Y.; Ibuka, T.; Yamamoto, Y. *Chem. Commun.* **1994**, 2003.

Chart 2. Cu(II) Complexes of *N*-Confused Porphyrins

N-confused porphyrin acts as a complexing agent capable of stabilizing the copper(III) oxidation state.^{38,39} Several stable organometallic complexes of copper(III) were characterized by X-ray crystallography.^{38–42}

In contrast to Cu(I) and Cu(III), organocopper(II) complexes are extremely rare. Initially, the transient σ -alkyl adducts of Cu(II) were postulated to form in the reactions of Cu(I) complexes with aliphatic radicals obtained by pulse-radiolysis techniques.⁴³ Eventually, organocopper(II) compounds were synthesized by applying an efficient protection of the Cu(II)–C bond in the coordination (C3NN) core of *N*-confused porphyrin.²⁰ The combination of electron paramagnetic resonance (EPR) and ²H NMR yielded detailed insight into the electronic structure of these organocopper(II) species.²⁰ As a result of steric constraints imposed by the ligand geometry, the C(21) atom creates two distinctly different types of the Cu(II)–C(21) bond. Specifically, the equatorial macrocycle may act as an sp^2 σ -carboanion, e.g., (H)1-Cu(II) and (Me)1-Cu(II) (Chart 2). Alternatively, as illustrated by (Me)1Me-Cu(II)Cl, the *C*-methylated pyrrole seems to coordinate to the Cu in the η^1 -fashion but the coordinating C(21) atom preserves trigonal geometry.

Subsequently, Furuta and co-workers reported that *N*-confused porphyrin bearing pentafluorophenyl groups forms the square-planar structure as elucidated by X-ray analyses.²³

These authors discovered an interconversion between the Cu(II) and Cu(III) complexes of *N*-confused porphyrin, which is stimulated by the accompanying protonation/deprotonation of the perimeter N atom.⁴⁴ *N*-Confused porphyrin undergoes a Cu(II)-assisted degradation to afford aryl-substituted tripyrironone.⁴⁵ Formation of a Cu(II) *N*-confused porphyrin species is involved in the mechanism. Apart from *N*-confused porphyrin, the *N*-confused calix[4]pyriron acts as an organometallic ligand, which stabilizes rare organocopper(II) complexes.⁴⁶

As a part of our continuing program of investigating the organometallic chemistry of paramagnetic carborporphyrinoids, here we report on the synthesis and spectroscopic characterization of Cu(II) complexes of pyrrole-appended *O*-confused porphyrin. These studies explore new controlling macrocyclic factors that potentially are of importance in the emerging field of Cu(II) organometallic chemistry. The peculiar flexibility of the *O*-confused oxaporphyrin structure, expected to shape the stability and reactivity of the resulting Cu(II) and Cu(III) complexes, has been a matter of specific interest.

Results and Discussion

Cu Complexes of Pyrrole-Appended *O*-Confused Oxaporphyrin. The reaction of copper(II) acetate and **4** under mild conditions [tetrahydrofuran (THF), reflux, 30 min] resulted in quantitative formation of **4**-Cu(III) (Scheme 1).

The UV–vis spectrum of **4**-Cu(III) (Figure 1) presents the pattern typical for aromatic porphyrin derivatives with the intense Soret band, and the set of Q bands in the 350–700 nm region, comparable to the diamagnetic silver(III) *O*-confused oxaporphyrin complexes.⁹ The high values of

(35) Fernandez de la Pradilla, R.; Rubio, M. B.; Marino, J. P.; Viso, A. *Tetrahedron Lett.* **1992**, *33*, 4985.

(36) Nakamura, E.; Mori, S.; Morokuma, K. *J. Am. Chem. Soc.* **1997**, *119*, 4900.

(37) Krause, N.; Gerold, A. *Angew. Chem., Int. Ed.* **1997**, *36*, 186.

(38) Furuta, H.; Maeda, H.; Osuka, A. *J. Am. Chem. Soc.* **2000**, *122*, 803.

(39) Maeda, H.; Osuka, A.; Furuta, H. *J. Am. Chem. Soc.* **2003**, *125*, 15690.

(40) Eujen, H.; Hoge, B.; Brauer, D. *J. Organomet. Chem.* **1996**, *519*, 7.

(41) Neumann, D.; Roy, T.; Tebbe, K.-F.; Crump, W. *Angew. Chem., Int. Ed. Engl.* **1993**, *32*, 1482.

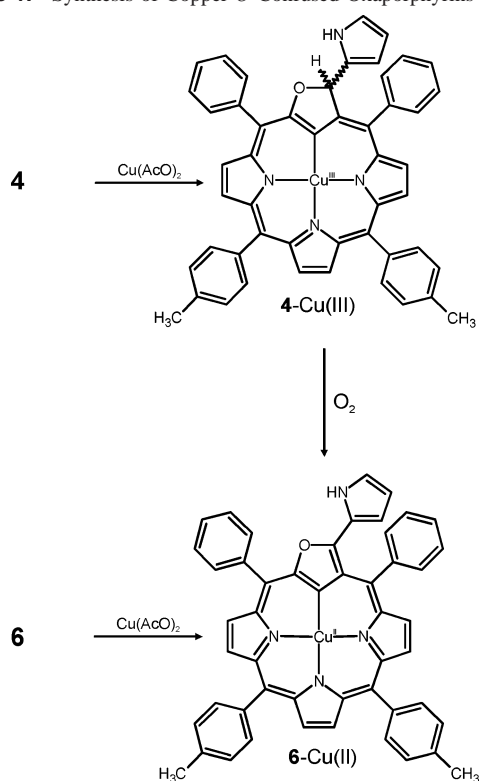
(42) Willert-Porada, M. A.; Burton, D. J.; Baenzinger, N. C. *Chem. Commun.* **1989**, 1633.

(43) Navon, N.; Golub, G.; Cohen, H.; Meyerstein, D. *Organometallics* **1995**, *14*, 5670.

(44) Maeda, H.; Ishikawa, Y.; Matsuda, T.; Osuka, A.; Furuta, H. *J. Am. Chem. Soc.* **2003**, *125*, 11822.

(45) Furuta, H.; Maeda, H.; Osuka, A. *Org. Lett.* **2002**, *4*, 181.

(46) Furuta, H.; Ishizuka, T.; Osuka, A.; Uwatoko, Y.; Ishikawa, Y. *Angew. Chem., Int. Ed.* **2001**, *40*, 2323.

Scheme 1. Synthesis of Copper *O*-Confused Oxaporphyrins

extinction coefficients observed for **4-Cu(III)** confirm the macrocyclic aromaticity.

The ^1H NMR spectrum of **4-Cu(III)** (Figure 2) illustrates the characteristic aromatic features of the species, which are consistent with the electronic spectrum. The NMR data comply with the tetrahedral geometry around C(3) characteristic for **4**, which is preserved after coordination.⁹ The presence of H(3) was confirmed indirectly with help of a ^1H – ^{13}C NMR correlation experiment.

The heteronuclear multiple-quantum coherence (HMQC) map allowed one to identify the C(3) signal at 86.9 ppm, which remains in good agreement with the previously observed ^{13}C NMR chemical shift (85.3 ppm) of the tetrahedral C atom determined for **4**. A characteristic pattern of the pendant pyrrole ring resonances was also observed.

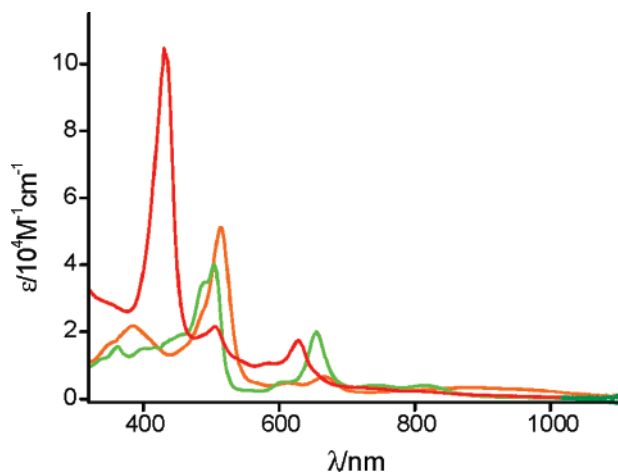


Figure 1. UV-vis spectra for **4-Cu(III)** (red), **6-Cu(II)** (green), and **8** (orange).

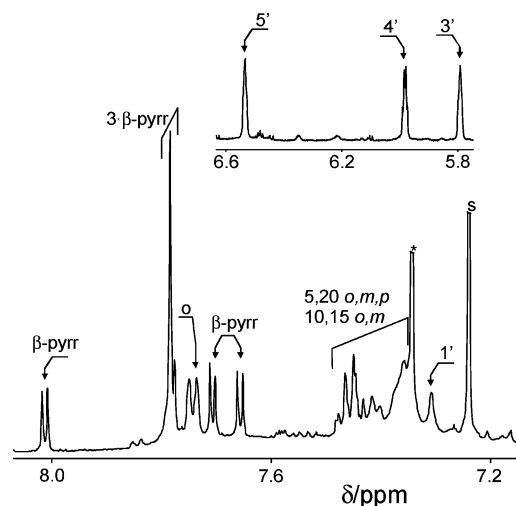


Figure 2. ^1H NMR spectrum of **4-Cu(III)** (CDCl_3 , 298 K). The inset presents resonances of the pendant pyrrole ring. Peak labels denote proton groups: pyr-H pyrrole; *o*, *m*, and *p* are ortho, meta, and para positions of meso-aryls (Ph and Tol), respectively.

The $\beta\text{-H}$ resonances of **4-Cu(III)** are observed in the region 8.1–7.6 ppm (Figure 1). In comparison to the structurally analogous silver(III) *O*-confused oxaporphyrin, the $\beta\text{-H}$ resonances of **4-Cu(III)** are relocated slightly upfield as the respective resonances of **4-Ag(III)** are placed at the 8.8–8.3 ppm region.⁹ In contrast, isoelectronic Ag(III)–Cu(III) *N*-confused complexes reveal very similar spectroscopic features ($\beta\text{-H}$: 9.5–8.6 ppm).^{19,44} The electronic structure of **4-Cu(III)** can actually be described by the resonance between two canonic forms ($\text{P}^3\text{-Cu(III)} \leftrightarrow \text{P}^2\text{-Cu(II)}$), where the second one brings around the paramagnetic contribution reflected by the described differences in the chemical shifts of **4-Cu(III)** and **4-Ag(III)**. An analogous situation was previously observed for metallotriarylcporroles. The $\beta\text{-H}$ resonances are in the region typical for aromatic compounds (9.20–8.10 ppm) when the Ag(III) ion is bound,⁴⁷ while a structurally similar Cu(III) complex presents their pyrrolic lines in the 7.9–7.3 ppm region.^{48,49} A striking example of such a difference was reported by Pacholska et al. for heterobimetallic face-to-face bis(corrole) systems.⁵⁰ There a simultaneous coordination of Cu(III) and Ag(III) yielded two sets of $\beta\text{-H}$ signals, which were easily assigned to Ag(III) (9.0–8.4 ppm) and Cu(III) (7.7–6.8 ppm) subunits.

We found that the **4-Cu(III)** species is extremely unstable in aerobic conditions. In the presence of dioxygen, **4-Cu(III)** readily undergoes a spontaneous conversion to form a paramagnetic Cu(II) compound **6-Cu(II)**, where the metal ion is bonded to three N atoms and one C atom of an inverted furan. As shown in Scheme 1, the profound rearrangement of the macrocyclic structure from **4** to **6** takes place, which

(47) Brückner, C.; Barta, C. A.; Briñas, R. P.; Krause Bauer, J. A. *Inorg. Chem.* **2003**, *42*, 1673.

(48) Will, S.; Lex, J.; Vogel, E.; Schickler, H.; Gisselbrecht, J.-P.; Hauptman, C.; Bernard, M.; Gross, M. *Angew. Chem., Int. Ed.* **1997**, *36*, 357.

(49) Brückner, C.; Brinas, R. P.; Krause-Bauer, J. A. *Inorg. Chem.* **2003**, *42*, 4495.

(50) Pacholska, E.; Espinoza, E.; Guillard, R. *Dalton Trans.* **2004**, 3181.

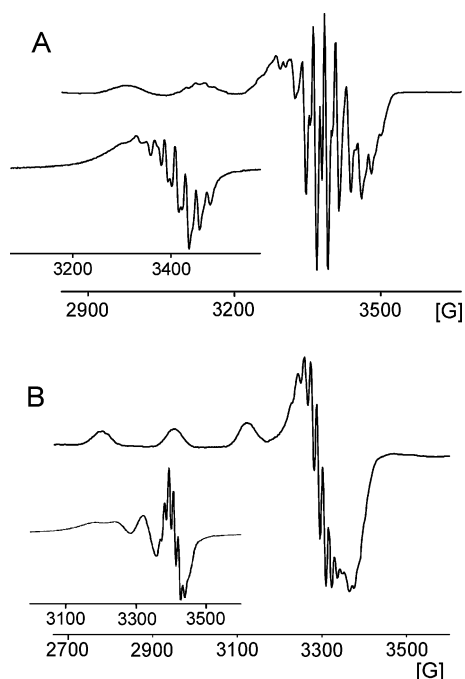


Figure 3. EPR spectra [X band, dichloromethane/toluene (80/20), 77 K]: (A) **6-Cu(II)** (microwave frequency 9.5851, microwave power 40 mW, modulation amplitude 7.73 G, modulation frequency 100 kHz); (B) **8** (microwave frequency 9.4277, microwave power 40 mW, modulation amplitude 6.81 G, modulation frequency 100 kHz). Insets in both traces present the corresponding isotropic spectra at 298 K.

is permitted through the already established flexibility of the inverted oxaporphyrin.⁹ Previously, we have observed these two different coordination modes correlated with a central metal oxidation state albeit never for the same element. A direct insertion of Cu(II) into **6** produced **6-Cu(II)** with a quantitative yield. The Cu(II) *O*-confused complex presents the UV–vis spectra (Figure 1) comparable to those of **6-Ni(II)** and **6-Pd(II)**, as expected for the metal(II) ions within a similar macrocyclic environment.⁹

The EPR spectra recorded for **6-Cu(II)** are presented in Figure 3. The isotropic ^{63,65}Cu hyperfine constants (Table 1) are relatively small when compared to the copper(II) porphyrins⁵¹ and copper(II) monoheteroporphyrins^{10,52–54} although similar to those determined for copper(II) dioxaporphyrin.⁵⁴ However, these values are comparable to the data of copper(II) *N*-confused porphyrin.^{20,55}

The absolute values of the spin-Hamiltonian parameters determined for anisotropic spectra of frozen solutions do not differ from those obtained for typical Cu(II) complexes.⁵⁶ This fact indicates that the orbital containing unpaired electrons (SOMO) involves a predominant metal contribution.

The UV–vis titration of **6-Cu(II)** with Br₂ results in one-electron oxidation to produce Cu(III) species **6-Cu(III)** (Chart

3). The electronic spectrum of **6-Cu(III)** is completely different from starting **6-Cu(II)** resembling that of Ag(III) inserted in **6**, i.e., **6-Ag(III)** (Figure 4).⁹

The spectrum shows the intense Soret-like band at 496 nm accompanied by comparable ones at 662 and 750 nm. Previously, we have demonstrated that the peculiar flexibility of pyrrole-appended oxacarborporphyrin is capable of stabilizing metal(II) (Ni(II) and Pd(II)) or metal(III) (Ag(III)) ions by fine adjusting of its own molecular/electronic structure.^{9,31} Accordingly, the appended pyrrole ring incorporation into the π -delocalization pathway can be tuned. Consequently, the charge of the macrocyclic cavity varies from -2 to -3 , fitting the requirements of the coordinated metal ion, in this particular case a Cu(II)–Cu(III) couple.

Crystal Structure of 6-Cu(II). The structure of **6-Cu(II)** has been determined by X-ray crystallography. The *O*-confused Cu(II) complex **6-Cu(II)** crystallizes in space group *P2₁/c*. The overall geometry observed for **6-Cu(II)** is presented in Figure 5. The macrocycle is only slightly distorted from planarity. The dihedral angle between the macrocyclic and pyrrole-appended planes reflects the biphenyl-like arrangement and equals 23.8°, with the NH group pointing toward the adjacent phenyl ring on the 5 position. This value is comparable to the previously reported one (26.4°) observed for crystal structure of a Ni(II) complex of pyrrole-appended *O*-confused oxaporphyrin **6-Ni(II)**.⁹ This angle is significantly smaller than the dihedral angles between the *meso*-aryl rings and the oxacarborporphyrin plane [phenyl(5) 66.9°, phenyl(20) 58.0°, *p*-tolyl(10) 64.0°, and *p*-tolyl(15) 55.3°]. For comparison, a coplanar arrangement of pyrrole and furan rings was reported for unsubstituted simple 2-(2'-furyl)pyrrole in solution.^{57,58}

The Cu(II)–N distances in **6-Cu(II)** [Cu–N(22) 2.020(3) Å, Cu–N(23) 1.977(3) Å, and Cu–N(24) 2.065(3) Å] are comparable to those in the nearly planar copper(II) porphyrins⁵⁹ or copper(II) octaethyl-5-oxaporphyrin.⁶⁰ The Cu(II)–C(21) bond length equals 1.939(4) Å. There are only two other reported examples of X-ray analysis on organometallic Cu(II) complexes characterized. The Cu(II)–N and Cu(II)–C(21) distances found for copper(II) *N*-confused calix[4]-porphyrin [Cu(II)–C(21) 2.007(4) Å, Cu(II)–N(22) 2.076(4) Å, Cu(II)–N(23) 2.010(3) Å, and Cu(II)–N(24) 2.056(4)] are slightly longer than those reported for **6-Cu(II)**, which may be related to the differences in the extent of conjugations encountered in both macrocycles. Copper(II) *N*-confused porphyrin bearing pentafluorophenyl groups forms a square-planar structure as elucidated by X-ray analyses. The average bond lengths between Cu(II) and ligand atoms are 1.980(9) and 2.018(9) Å,²³ but the crystal structure disorder excludes the detailed bond length discussion.

(51) Brown, T. G.; Hoffman, B. M. *Mol. Phys.* **1980**, *39*, 1073.

(52) Latos-Grażyński, L.; Jezierski, A. *Inorg. Chim. Acta* **1985**, *1985*, 106.

(53) Lisowski, J.; Grzeszczuk, M.; Latos-Grażyński, L. *Inorg. Chim. Acta* **1989**, *161*, 153.

(54) Sridevi, B.; Narayanan, S. J.; Srinivasan, A.; Chandrashekar, T. K.; Subramanian, J. *J. Chem. Soc., Dalton Trans.* **1998**, 1979.

(55) Mitrikas, G.; Calle, C.; Schweiger, A. *Angew. Chem., Int. Ed.* **2005**, *3301*.

(56) Hathaway, B. J. *Struct. Bonding (Berlin)* **1984**, *37*, 55.

(57) Orti, E.; Sanchez-Marin, J.; Merchan, M.; Tomas, F. *J. Phys. Chem.* **1987**, *91*, 545.

(58) Gallaso, V.; Klasinic, L.; Sabljic, A.; Trinajstic, N.; Pappalardo, G. C.; Steglich, W. *J. Chem. Soc., Perkin Trans. 2* **1981**, 127.

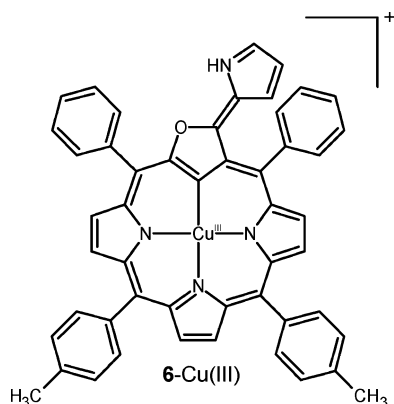
(59) Scheidt, W. R.; Reed, C. R. *Chem. Rev.* **1981**, *81*, 543.

(60) Koerner, R.; Olmstead, M. M.; Ozarowski, A.; Phillips, S. L.; Van Calcar, P. M.; Winkler, K.; Balch, A. L. *J. Am. Chem. Soc.* **1998**, *120*, 1274.

Table 1. Spin-Hamiltonian Parameters of Cu(II) Complexes of *O*-Confused Oxaporphyrins

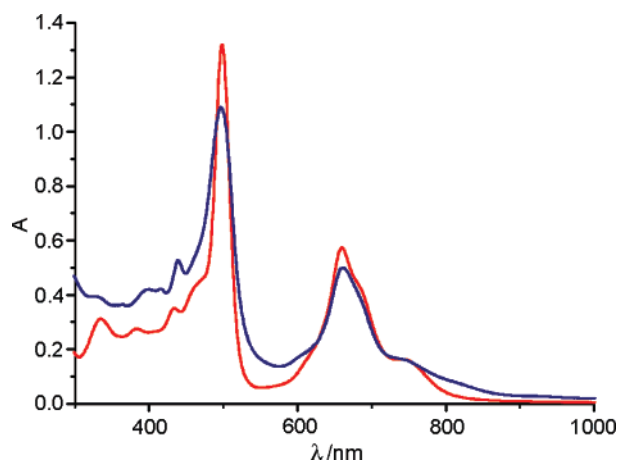
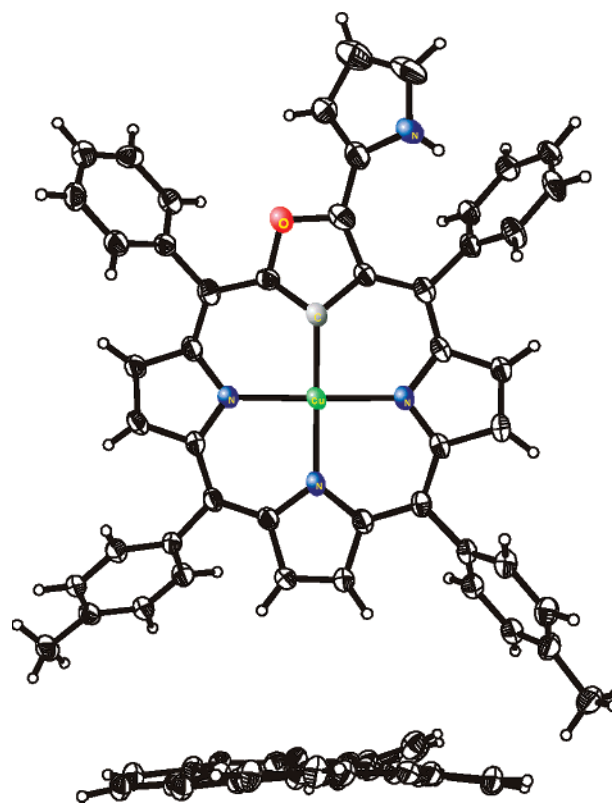
compound	$-A_{\parallel}^{\text{Cu}}$	$-A_{\perp}^{\text{Cu}}$	g_{\parallel}	g_{\perp}	$-A_{\text{o}}^{\text{Cu}}$	g_{o}	$-A_{\text{o}}^{\text{N}}$	ref
6-Cu(II) ^a	154	-29	2.134	2.029	30	2.073	21.6	this paper
8 ^b	169	30.6	2.218	2.046	76.8	2.086	13.2	this paper
(H) 1 -Cu(II)	143	-37	2.139	2.057	23	2.070	18.3	20
(Me) 1 -Cu(II)	140	-27	2.142	2.054, 2.026	28.5	2.079	20.0	20
(H) 1H -Cu(II)Cl	154	13	2.190	2.050	60.0	2.110	13.0	20
(Me) 1H -Cu(II)Cl	151	13	2.195	2.052	59.2	2.113	12.9	20

^a The ¹⁴N hyperfine constant in the perpendicular region is 22.3, 13.1 and that in the parallel region is 18.7. ^b The ¹⁴N hyperfine constant in the perpendicular region is 13.8.

Chart 3

Reactivity of 6-Cu(II) toward Dioxygen. Copper(II) *O*-confused oxaporphyrin with appended pyrrole ring **6-Cu(II)** dissolved in CHCl_3 undergoes reactions with dioxygen over a period of hours. The complex **6-Cu(II)** was predominantly ring-opened through oxidative cleavage to form the open-chain copper(II) tripyrrole species identified as copper(II) 14-benzoyl-5,10-bis(*p*-tolyl)-1-oxotripyrrole complex **7a** (Scheme 2).

In the course of oxygenolysis, the *O*-confused furan fragment with an appended pyrrole ring and the adjacent $\text{C}_6\text{H}_5\text{-C}_{\text{meso}}$ units have been extruded. The cleavage of **6-Cu(II)** has been accompanied by oxygenation of **6-Cu(II)** at the C(21) position, which led to the formation of copper(II) 5,20-diphenyl-10,15-ditolyl-2-oxa-3-(2'-pyrrolyl)-21-hydroxycarbaporphyrinatocopper(II) (**8**) albeit in a relatively low yield. This species has been found to be, contrary to **6-Cu(II)**, resistant to cleavage at the meso positions. Thus, in the course of this process, a new type of core-modified porphyrin

**Figure 4.** UV-vis spectra for **6-Cu(III)** (blue) and **6-Ag(III)** (red).**Figure 5.** Crystal structure of **6-Cu(II)**. The upper trace presents a perspective view and the bottom one a side view (aryl substituents are omitted for clarity).

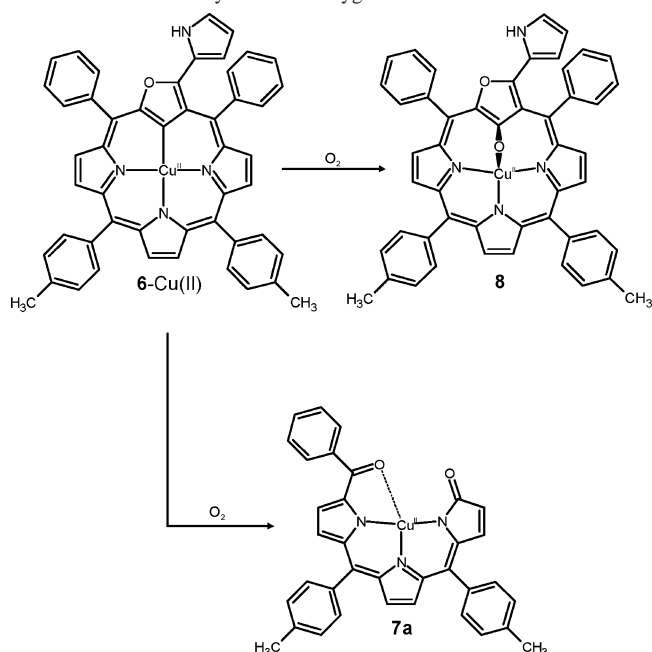
has been identified. The macrocycle incorporates 3-hydroxyfuran into the porphyrin-like structure. Both compounds are stable and have been purified by the standard chromatographic procedures.

Identification of **7a** has been facilitated because an identical complex was previously isolated and fully characterized by Furuta and co-workers as a degradation product of *N*-confused porphyrins in the presence of Cu(II).⁴⁵ Thus, the spectroscopic features of **7a** matched those of copper(II) tripyrrole formed from copper(II) *N*-confused porphyrin.⁴⁵

In order to explore the regioselectivity of oxidative degradation, an analogue of **4a**, i.e., 20-phenyl-5,10,15-tritolyl-2-oxa-3-hydro-3-(2'-pyrrolyl)-21-carbaporphyrin (**4b**), was synthesized. The oxidative degradation afforded two feasible copper(II) tripyrrole complexes, **7a** and **7b** (70:30; Scheme 3), as was unambiguously confirmed by mass spectra [**7a**, m/z 583.2 ($\text{M} + \text{H}$)⁺; **7b**, m/z 597.2 ($\text{M} + \text{H}$)⁺].

In the case of degradation of copper(II) *N*-confused porphyrin, the specific substitution at the meso position by 2-pyridyl resulted in a regioselective extrusion.⁴⁵ The first

Scheme 2. Reactivity toward Dioxygen



step of oxygenolysis involved the C_{α} - C_{meso} bond adjacent to the N atom of the *N*-confused pyrrole ring. The cleaved *meso*-phenyl moiety was located next to the β -C of the same ring. The determined difference of the regioselectivities of copper(II) *N*- and *O*-confused porphyrins may reflect a difference in the nature of the *X*-confused ring and/or in the choice of *meso*-aryl substituents. Presumably, the 2-pyridyl moiety favors cleavage of the C_{α} - C_{meso} (2-pyridyl) bond in the first oxygenolysis step in comparison to the alternative C_{α} - C_{meso} (phenyl) one. The steric/electronic factor introduced in the case investigated here seems not to be essential, considering the minor differences in the structures of *meso* substituents adjacent to the *O*-confused ring, which are, however, sufficient to distinguish two feasible products.

The degradation of copper(II) *N*- and *O*-confused porphyrins can be considered as a peculiar case of dioxygen activation in the porphyrin-like environment. Contrary to *N*- and *O*-confused derivatives, regular copper(II) porphyrins are relatively stable toward dioxygen. In this context, it is essential to recall that copper(II) octaethyl(*meso*-hydroxy)porphyrins, (OEPOH)Cu(II), undergo oxidation by dioxygen to form a dinuclear Cu(II) complex that is composed of a copper(II) *meso*-substituted porphyrin portion that is attached through an ester linkage to a helical copper(II) tetrapyrrole that has been ring-opened through oxidative cleavage of a second molecule of (OEPOH)Cu(II).⁶¹ This oxidative ring-opening reaction resembles that of natural heme catabolism.⁶⁰ Independently synthesized Cu(II) complexes of octaethylbilindione react with dioxygen, which results in cleavage of the tetrapyrrolic ligand to form a Cu(II) complex containing a propentdyopent class dipyrrole.⁶²

21-Hydroxy *O*-Confused Oxaporphyrin. The reaction of 6-Cu(II) with hydrogen peroxide, performed under

heterophasic conditions, resulted in quantitative, regioselective hydroxylation centered at the internal C(21) atom (Scheme 4).

A specific reactivity of metallocarborporphyrinoids centered on internal C-H or C-M units was previously reported. For instance, *m*-benzporphyrin undergoes selective acetoxylation, chlorination, or pyridination.^{26,28,63} The iron and manganese *N*-confused porphyrin react with dioxygen. As a consequence, 2-azacarborporphyrin acquires oxofunctionality [C(21)O] in the coordination core.^{64,65} Finally, an attempt to insert Cu(II) into azuliporphyrin afforded a Cu(II) complex, where the Cu(II) ion is bounded by three N atoms and the O atom of the 21-hydroxy group.⁶⁶ The EPR spectrum recorded for 8 (Figure 3, trace B, and Table 1) presents a pattern clearly different from that of the hydroxylation substrate 6-Cu(II), but it resembles those of copper(II) *N*-confused porphyrin complexes, where the C(21) atom was protonated.²⁰

Treatment of 8 with acid results in demetalation to form 21-hydroxy derivative 9 (Scheme 4). Significantly, for the structural conclusions, the reversed process, i.e., insertion of Cu(II) into 9, gives 8 quantitatively. Previously, a keto-enol tautomerization has been observed for a group of hydroxylated derivatives derived from *N*-confused porphyrin,⁶⁵ *m*-benzporphyrin,⁶⁷ and azuliporphyrin.⁶⁶ On the contrary, the 21-hydroxycarborporphyrinoid structure is entirely preferred for 9. Presumably, the presence of appended pyrrole and O at the macrocycle perimeter effectively blocks any possibility of transformation into a keto tautomer of 9. The ¹H NMR spectrum of 9 (Figure 6) contains three AB systems assigned to the β -pyrrolic protons [H(7) 7.25, H(8) 6.69 (³*J* = 4.5 Hz); H(13) 6.92, H(12) 6.70 (³*J* = 4.6 Hz); H(18) 6.72, H(17) 6.59 (³*J* = 4.6 Hz)]. The complete assignment was performed on the basis of several two-dimensional experiments (COSY, NOESY, HMQC, and HMBC). Two broad resonances at 11.49 and 8.87 ppm were identified as NH and OH signals, respectively. The COSY experiment at low temperature (220 K), where scalar couplings between already assigned β -H's and an appropriate NH resonance allowed the unambiguous localization of the NH hydrogen. The spectral range observed for 9 suggests that the macrocyclic π -delocalization pathway is blocked. Thus, the macrocyclic aromaticity is lowered. This is the first example of an *O*-confused porphyrin where the β -H resonances are located in the region typical for heterocyclic aromaticity of its five-membered components. The previously described macrocycles with an inverted furan ring present delocalization that results in downfield-shifted signals of β -H's.^{8,9,31} However, nonaromatic structures as reflected by the characteristic chemical shift values were observed for

(63) Stępień, M.; Latos-Grażyński, L. *Org. Lett.* **2003**, *5*, 3379.

(64) Hung, C.-H.; Chen, W.-C.; Lee, G.-H.; Peng, S.-M. *Chem. Commun.* **2002**, 1516.

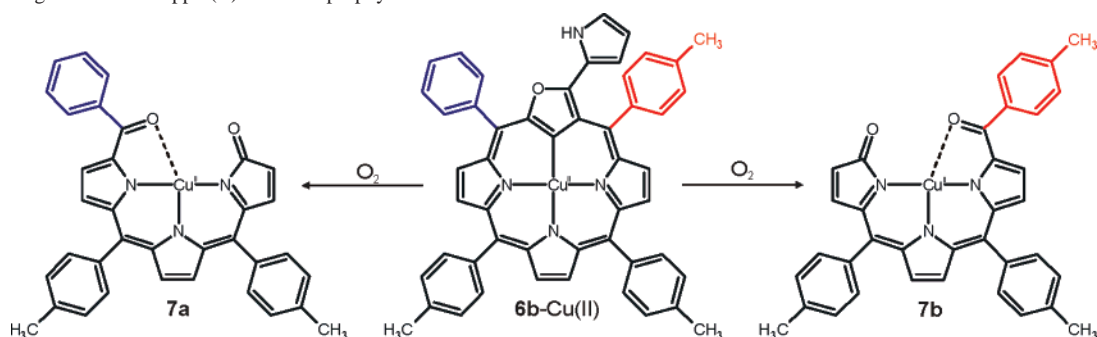
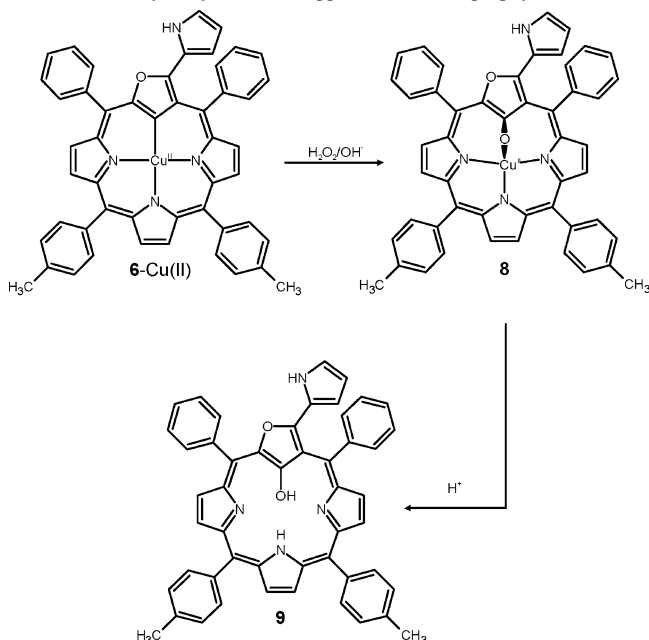
(65) Hung, C.-H.; Wang, S.-L.; Ko, J.-L.; Peng, C.-H.; Hu, C.-H.; Lee, M.-T. *Org. Lett.* **2004**, *6*, 1393.

(66) Colby, D. A.; Ferrence, G. M.; Lash, T. D. *Angew. Chem., Int. Ed.* **2004**, *43*, 1346.

(67) Stępień, M.; Latos-Grażyński, L.; Sztrenberg, L. *J. Org. Chem.* **2007**, *72*, 2259.

(61) Phillips, S.; Noll, B. C.; Olmstead, M. M.; Balch, A. L. *Can. J. Chem.* **2001**, *79*, 922.

(62) Balch, A. L.; Mazzanti, M.; Noll, B. C.; Olmstead, M. M. *J. Am. Chem. Soc.* **1993**, *115*, 12206.

Scheme 3. Degradation of Copper(II) Oxacarborphyrin**Scheme 4.** Hydroxylation of Copper(II) Oxacarborphyrin

S-confused thiaporphyrin,⁵ *m*-benzporphyrin,²⁸ and 3-aza-*m*-benzporphyrin (*N*-confused pyriporphyrin).⁶⁸

Conclusion

Thus, this work revealed that an *O*-confused porphyrin with an appended pyrrole ring offers a unique macrocyclic environment in which to form organocopper compounds and to control their reactivity. In particular, the specific routes to tuning carbaporphyrinoid properties, according to the

requirements of Cu ions, via a modification centered at the 2-(2'-furyl)pyrrole moiety, have been explored. Thus, the present investigations offer evidence for stabilization of unusual organocopper(II) species via the very efficient protection of the Cu(II)–C bond by encapsulating the coordinated Cu(II) center in the core of 2-oxa-21-carbaporphyrin (NNNC). The true *O*-confused porphyrin readily accommodates Cu(II), as confirmed by EPR parameters. Significantly, the crystallographic analysis confirms the formation of the short Cu(II)–C bond [1.939(4) Å] because the equatorial macrocycle acts similarly to an sp² σ-carbanion.

One can realize that the oxidative ring opening of copper(II) *O*-confused oxaporphyrin to form a copper(II) tripyrriponone complex in the presence of dioxygen and the regioselective C(21) hydroxylation can be related to heme degradation that utilizes dioxygen with heme oxygenase or coupled oxidation conditions.^{69,70} It was previously shown that heme degradation can proceed beyond the ring opening that produces an iron biliverdin complex as well as verdoheme. For instance, octaethylverdoheme and iron biliverdin complexes are converted into iron(III) hexaethyltripyrone.⁷¹ The reaction of (*meso*-NH₂OEP)Fe(II)(Py)₂ with dioxygen produced a metastable, ring-opened tetrapyrrole that has been oxygenated at a second meso position and that served as a model for the oxidative removal of the terminal pyrrole group.⁷¹ In this context, the mechanistic aspects of the process of cleavage of copper(II) *O*-confused oxaporphyrin and in particular its relevance to the coupled oxidation mechanism are of current interest.

Experimental Section

Solvents and Reagents. Dichloromethane-*d*₂ (CIL) was used as received. Chloroform-*d* (CIL) was passed through basic Al₂O₃. Macrocytes **4a** and **6** were obtained as previously described.^{9,31}

20-Diphenyl-5,10,15-tritolyl-2-oxa-3-hydro-3-(2'-pyrrolyl)-21-carbaporphyrin (4b). Macrocycle **4b** was obtained by a previously described procedure⁹ using 2-phenylhydroxymethyl-4-*p*-tolylhydroxymethylfuran as a source of the inverted furan. UV–vis (CH₂-Cl₂, λ_{max}/nm (log ε)): 439 (5.37), 534 (4.30), 569 (4.16), 622 (3.98),

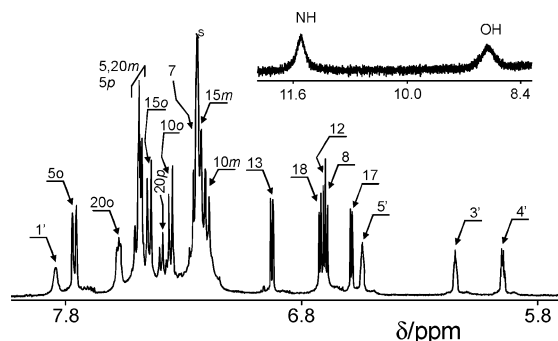


Figure 6. ¹H NMR spectrum of **9** (CDCl₃, 298 K). The inset presents the downfield region with NH and OH protons. Peak labels follow systematic position numbering of the macrocycle or denote proton groups: *o*, *m*, and *p* are ortho, meta, and para positions of *meso*-aryls (Ph and Tol), respectively.

(68) Mysliborski, R.; Latos-Grażyński, L. *Eur. J. Org. Chem.* **2005**, 5039.

(69) Balch, A. L.; Latos-Grażyński, L.; Noll, B. C.; Olmstead, M. M.; Safari, N. *J. Am. Chem. Soc.* **1993**, *115*, 9056.

(70) Kalish, H.; Latos-Grażyński, L.; Balch, A. L. *J. Am. Chem. Soc.* **2000**, *122*, 12478.

(71) Kalish, H.; Lee, H. M.; Olmstead, M. M.; Latos-Grażyński, L.; Rath, S. P.; Balch, A. L. *J. Am. Chem. Soc.* **2003**, *125*, 4674.

680 (4.25). ^1H NMR (CDCl_3 , 298 K): δ 8.49 (d, 1H, $^3J = 4.6$ Hz), 8.47 (d, 1H, $^3J = 4.6$ Hz), 8.46 (d, 1H, $^3J = 4.6$ Hz), 8.44 (d, 1H, $^3J = 4.6$ Hz), 8.43 (d, 1H, $^3J = 4.6$ Hz), 8.28 (d, 1H, $^3J = 4.6$ Hz), 8.11 (m, 2H), 8.05 (s, 1H), 8.04 (m, 2H), 7.99 (m, 1H), 7.90 (bs, 1H), 7.67–7.63 (m, 2H), 7.55 (tt, 1H), 7.52–7.45 (m, 5H), 7.41 (bs, 1H), 7.20 (bs, 1H), 7.16 (bs, 1H), 7.14 (bs, 1H), 6.30 (m, 1H), 5.82 (m, 1H), 5.50 (m, 1H), 2.66 (s, 3H), 2.65 (s, 3H), 2.54 (s, 3H), –1.34 (bs, 2H), –5.07 (s, 1H). ^{13}C NMR (CDCl_3 , 298 K): δ 160.2, 152.9, 152.4, 143.6, 140.1, 139.3, 139.29, 139.2, 138.4, 137.5, 137.3, 137.2, 137.0, 135.1, 134.4, 134.3, 134.2, 134.04, 134.0, 133.8, 133.6 (bs), 132.1, 131.8, 130.8 (bs), 130.2, 128.6 (bs), 127.8, 127.6, 127.5, 127.2, 126.3, 126.2, 123.1, 123.0, 121.1, 120.2, 117.7, 112.6, 109.1, 108.2, 106.5, 106.4, 105.1, 85.2, 21.5, 21.5, 21.4. HRMS: m/z_{calc} 724.3170 (calcd 724.3202 for $\text{C}_{51}\text{H}_{40}\text{N}_4\text{O}$).

5,20-Diphenyl-10,15-ditoly-2-oxa-3-hydro-3-(2'-pyrrolyl)-21-carbaporphyrinatocopper(III) (4-Cu(III)). The mixture of **4** (20 mg, 0.03 mmol) and $\text{Cu}(\text{AcO})_2 \cdot 2\text{H}_2\text{O}$ (10 mg, 0.046 mmol) was dissolved in 20 mL of freshly distilled THF. The resulting mixture was refluxed for 30 min and evaporated to dryness with a vacuum rotary evaporator. The remaining solid was dissolved in a small volume of freshly distilled CH_2Cl_2 and filtered from an inorganic salt. The reaction is quantitative and does not require recrystallization. UV–vis (CH_2Cl_2 , $\lambda_{\text{max}}/\text{nm}$ (log ϵ): 433 (5.02), 506 (4.33), 628 (4.24). ^1H NMR (CDCl_3 , 298 K): δ 8.01 (d, 1H, $^3J = 4.9$ Hz), 7.79–7.77 (m, 4H), 7.74 (m, 2H), 7.71 (d, 1H, $^3J = 4.6$ Hz), 7.65 (d, 1H, $^3J = 4.9$ Hz), 7.48–7.43 (m, 5H), 7.42–7.39 (m, 3H), 7.38–7.32 (m, 8H), 7.31 (bs, 1H), 6.53 (m, 1H), 5.98 (m, 1H), 5.79 (m, 1H), 2.53 (s, 3H), 2.52 (s, 3H). ^{13}C NMR (CDCl_3 , 298 K, partial data): δ 133.3, 133.0, 132.9, 131.0, 129.6, 129.0, 128.8, 128.4, 128.3, 127.7, 124.8, 87.2, 21.8.

5,20-Diphenyl-10,15-ditoly-2-oxa-3-(2'-pyrrolyl)-21-carbaporphyrinatocopper(II) (6-Cu(II)). The mixture of **6** (13 mg, 0.018 mmol) and $\text{Cu}(\text{AcO})_2 \cdot 2\text{H}_2\text{O}$ (12 mg, 0.056 mmol) was dissolved in 20 mL of freshly distilled THF. The resulting mixture was stirred for 5 min and evaporated to dryness with a vacuum rotary evaporator. The remaining solid was dissolved in a small volume of freshly distilled CH_2Cl_2 and filtered from an inorganic salt. The reaction is quantitative and does not require further purification. UV–vis (CH_2Cl_2 , $\lambda_{\text{max}}/\text{nm}$ (log ϵ): 363 (4.19), 402 (4.18), 487 (sh), 505 (4.60), 608 (3.71), 655 (4.30), 743 (3.60), 815 (3.60). MS: m/z_{calc} 769.2154 (calcd 769.2128 for $\text{C}_{50}\text{H}_{36}\text{N}_4\text{O}^{63}\text{Cu}$).

5,20-Diphenyl-10,15-ditoly-2-oxa-3-(2'-pyrrolyl)-21-hydroxy-carbaporphyrinatocopper(II) (8). A total of 15 mg (0.27 mmol) of KOH was dissolved in 20 mL of water and mixed with 30 mL of H_2O_2 (30%). The resulting mixture was added to **6-Cu(II)** (10 mg, 0.015 mmol) dissolved in 20 mL of freshly distilled CH_2Cl_2 . Whole mixture was stirred overnight and washed with water (2 \times). The organic layer was passed through a chromatography column with Al_2O_3 (base, GIV). A fast-moving orange band was collected to give **8** with quantitative yield. UV–vis (CH_2Cl_2 , $\lambda_{\text{max}}/\text{nm}$ (log ϵ): 348 (sh), 384 (4.34), 515 (4.71), 613 (3.67), 667 (3.82), 880 (3.52), 959 (sh). HRMS: m/z_{calc} 785.2012 (calcd 785.1978 for $\text{C}_{50}\text{H}_{34}\text{N}_4\text{O}_2^{63}\text{Cu}$).

5,20-Diphenyl-10,15-ditoly-2-oxa-3-(2'-pyrrolyl)-21-hydroxy-porphyrin (9). **8** (10 mg, 0.013 mmol) was dissolved in 15 mL of ethyl acetate. Then gaseous HCl was passed through the solution to initiate a distinct color change from orange to violet. The resulting mixture was chromatographed with Al_2O_3 (GIV) suspended in CH_2Cl_2 . A fast-moving orange fraction was collected. The solvent was removed with a vacuum rotary evaporator. Recrystallization with CH_2Cl_2 /hexane gave **9** in quantitative yield. UV–vis (CH_2Cl_2 , $\lambda_{\text{max}}/\text{nm}$ (log ϵ): 381 (3.60), 500 (3.61). ^1H NMR (CDCl_3 , 298 K): δ 11.49 (bs, NH), 8.87 (bs, OH), 7.84 (bs, NH), 7.61 (m, 2H), 7.57

Table 2. Crystal Data for **6-Cu(II)** with Refinement Details

compound	6-Cu(II)
crystals grown by	slow diffusion of methanol into a CH_2Cl_2 solution
crystal habit	dark-green block
formula	$\text{C}_{50}\text{H}_{34}\text{N}_4\text{OCu}$
fw	770.35
<i>a</i> , Å	10.321(2)
<i>b</i> , Å	23.474(5)
<i>c</i> , Å	14.752(3)
β , deg	97.608(15)
<i>V</i> , Å ³	3542.6(12)
<i>Z</i>	4
<i>D</i> _{calc} , g·cm ^{−3}	1.444
cryst syst	monoclinic
space group	<i>P</i> 2 ₁ / <i>c</i>
μ , mm ^{−1}	1.240
abs corr	analytical (0.880/0.976)
<i>T</i> , K	100(2)
θ range	3.56 $\leq \theta \leq$ 70.78
<i>hkl</i> range	−11 $\leq h \leq$ 9, −29 $\leq k \leq$ 23, −15 $\leq l \leq$ 18
reflections	
measd	26 953
unique, $I \geq 2\sigma(I)$	6435
param/restraints	502/0
<i>S</i>	0.781
R1	0.0474
wR2	0.1223

(m, 2H), 7.51–7.46 (m, 9H), 7.44 (d, 2H, $^3J = 8.0$ Hz), 7.39 (m, 1H), 7.35 (d, 2H, $^3J = 8.0$ Hz), 7.25 (d, 1H, $^3J = 4.9$ Hz), 6.92 (d, 1H, $^3J = 4.6$ Hz), 6.72 (d, 1H, $^3J = 4.2$ Hz), 6.70 (d, 1H, $^3J = 4.6$ Hz), 6.69 (d, 1H, $^3J = 4.2$ Hz), 6.59 (d, 1H, $^3J = 4.6$ Hz), 6.54 (m, 1H), 6.15 (m, 1H), 5.95 (m, 1H), 2.45 (s, 3H), 2.44 (s, 3H). ^{13}C NMR (CDCl_3 , 298 K, partial data): δ 135.5 (C-13), 132.5 (C-5*o*), 132.4 (C-10*o*), 132.3 (C-12), 132.0 (C-20*o*), 131.8 (C-15*o*), 131.0, 128.9, 127.5 (C-5,20*m*,5*p*), 130.5 (C-8), 129.1 (C-7), 128.3 (C-15*m*), 128.7 (C-10*m*), 127.9 (C-20*p*), 125.9 (C-5'), 123.3 (C-18), 122.1 (C-17), 119.2 (C-3'), 111.2 (C-4'), 21.8 (2C-*p*-Me). MS: m/z_{calc} 724.2822 (calcd 724.2838 for $\text{C}_{50}\text{H}_{36}\text{N}_4\text{O}_2$).

Instrumentation. NMR spectra were recorded on a Bruker Avance 500 spectrometer (frequencies: ^1H NMR 500.13 MHz; ^{13}C NMR 125.77 MHz) equipped with either a broad-band inverse-gradient probehead or a direct broad-band probehead. Absorption spectra were recorded on a diode-array Hewlett-Packard 8453 spectrometer. Mass spectra were recorded on an AD-604 spectrometer using the electrospray and liquid matrix secondary-ion mass spectrometry techniques. EPR spectra were recorded on a Bruker ESP 300 spectrometer operating with an X band equipped with a ER 035M gaussmeter and a HP 53550B microwave frequency counter. The spectra were simulated using the *SYMFO-NIA* software package.

X-ray Analysis. X-ray-quality crystals of **6-Cu(II)** were prepared by diffusion of methanol into a dichloromethane solution contained in a thin tube stored in a refrigerator. Data were collected at 100 K on an Xcalibur PX k-geometry diffractometer, with Cu K α radiation ($\lambda = 1.5418$ Å). The data were corrected for Lorentz and polarization effects. An analytical absorption correction was applied. Crystal data are compiled in Table 2. The structure was solved by a heavy-metal method with *SHELXS-97* and refined by the full-matrix least-squares method by using *SHELXL-97* with anisotropic thermal parameters for the non-H atoms. Scattering factors were those incorporated in *SHELXS-97*.^{72,73}

(72) Sheldrick, G. M. *SHELXL97, Program for Crystal Structure Solution*; University of Göttingen: Göttingen, Germany, 1997.

Acknowledgment. Financial support from the Ministry of Science and Higher Education (Grant 3 T09A 162 28) is kindly acknowledged.

(73) Sheldrick, G. M. *SHELXL97, Program for Crystal Structure Refinement*; University of Göttingen: Göttingen, Germany, 1997.

Supporting Information Available: Tables of crystal data, bond lengths, angles, anisotropic thermal parameters (CIF files). This material is available free of charge via the Internet at <http://pubs.acs.org>.

IC700631T